

Exploring Transition Pathway and Free-Energy Profile of Large-Scale Protein Conformational Change by Combining Normal Mode Analysis and Umbrella Sampling Molecular Dynamics

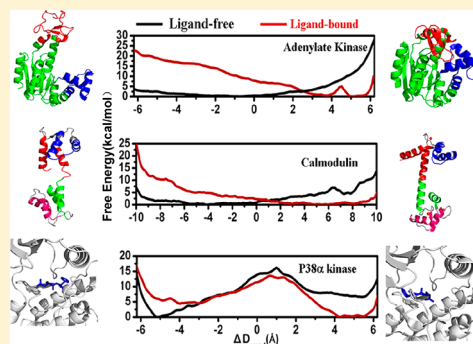
Jinan Wang,[†] Qiang Shao,^{*,†} Zhijian Xu,[†] Yingtao Liu,[†] Zhuo Yang,[†] Benjamin P. Cossins,[‡] Hualiang Jiang,[†] Kaixian Chen,[†] Jiye Shi,^{*,‡} and Weiliang Zhu^{*,†}

[†]Drug Discovery and Design Center, CAS Key Laboratory of Receptor Research, Shanghai Institute of Materia Medica, Chinese Academy of Sciences, 555 Zuchongzhi Road, Shanghai, 201203, China

[‡]UCB Pharma, Slough SL1 3WE, United Kingdom

Supporting Information

ABSTRACT: Large-scale conformational changes of proteins are usually associated with the binding of ligands. Because the conformational changes are often related to the biological functions of proteins, understanding the molecular mechanisms of these motions and the effects of ligand binding becomes very necessary. In the present study, we use the combination of normal-mode analysis and umbrella sampling molecular dynamics simulation to delineate the atomically detailed conformational transition pathways and the associated free-energy landscapes for three well-known protein systems, viz., adenylate kinase (AdK), calmodulin (CaM), and p38 α kinase in the absence and presence of respective ligands. For each protein under study, the transient conformations along the conformational transition pathway and thermodynamic observables are in agreement with experimentally and computationally determined ones. The calculated free-energy profiles reveal that AdK and CaM are intrinsically flexible in structures without obvious energy barrier, and their ligand binding shifts the equilibrium from the ligand-free to ligand-bound conformation (population shift mechanism). In contrast, the ligand binding to p38 α leads to a large change in free-energy barrier ($\Delta\Delta G \approx 7$ kcal/mol), promoting the transition from DFG-in to DFG-out conformation (induced fit mechanism). Moreover, the effect of the protonation of D168 on the conformational change of p38 α is also studied, which reduces the free-energy difference between the two functional states of p38 α and thus further facilitates the conformational interconversion. Therefore, the present study suggests that the detailed mechanism of ligand binding and the associated conformational transition is not uniform for all kinds of proteins but correlated to their respective biological functions.



■ INTRODUCTION

The current view of protein structure now includes a realization that proteins continually undergo complex and hierarchical conformational changes while carrying out their biological functions, e.g., in signal transduction, immune response, protein folding, and enzymatic activity.¹ These conformational changes can be induced and/or modulated by the binding of ligands. Understanding how proteins interconvert from one conformation to another and the effects of ligand binding is crucial for elucidating their biological function.² Two theoretical models, namely, “induced fit” and “population shift” mechanisms, have been proposed to explore the molecular mechanism of protein conformational change and its correlation to ligand binding. In the first model, the conformational change was suggested as the direct consequence of ligand binding which drives the protein from the ligand-free (apo) conformation to that which is more complementary to the bound ligand.³ Thus, the two functional conformations of a protein can be converted only after the ligand binding. The “population shift” model, on the other hand, suggested that proteins are inherently dynamic and the

ligand binds selectively to an active conformation, shifting the equilibrium from the ligand-free conformation to ligand-bound conformation.^{4–6} To understand which model provides reasonable explanation for the conformational transition of a protein, the accurate evaluation of structural characteristics of intermediate conformations along the entire conformational transition pathway becomes necessary; however, this remains a challenging task for both experimental and theoretical approaches to date.

Experimental methods such as X-ray crystallography can solve the stable structures of proteins under a certain set of conditions, although this may not provide detailed information about dynamics. The application of real-time measurement techniques for protein motions is usually restricted by various factors, e.g., the time-resolved X-ray structural methods require that the studied molecule is inherently photosensitive or it

Received: October 24, 2013

Revised: December 17, 2013

Published: December 18, 2013

should be engineered to be so.^{7,8} The structure-dynamics information obtained from most experimental techniques are ensemble-averaged rather than the motion of individual molecules.⁹ Although nuclear magnetic resonance (NMR) can directly monitor kinetic information about the transition between different conformations, it is limited to relatively small protein systems.¹⁰

Molecular dynamics (MD) simulation can provide detailed dynamic information and thus has become an attractive additional approach.^{11–13} Low efficiency in sampling high-dimensional and rugged configuration spaces of proteins makes conventional MD simulation very computationally expensive. Therefore, many enhanced sampling methods have been developed to improve the sampling efficiency of MD simulation, including those that artificially add external driving force to guide the protein from one structure to another, such as the targeted MD simulation (TMD),¹⁴ and those that smooth the energy landscape with a biasing potential, such as accelerated MD,¹⁵ metadynamics,¹⁶ replica exchange MD (REMD),¹⁷ and so on. These methods could not only predict the pathway of protein conformational change but also calculate the free-energy landscape in the sampled conformational space, which is of central interest in understanding the mechanism of conformational change.^{18–20} However, the computed TMD pathway is biased force-dependent and its connection to function is unclear.²¹ Moreover, in all TMD algorithms, large-scale motions tend to precede small-scale motions.^{22,23} On the other hand, to obtain the accurate free-energy landscape, the computation of the potential biasing methods is too expensive.

Several coarse-grained methods have been developed to rapidly generate the protein conformational transition pathway without providing the energetic features of the conformational transition. The representative is the normal-mode analysis (NMA), which generates the low-frequency modes corresponding to the collective motions of a global protein by calculating the matrix of the second derivatives of the potential energy of the protein system.²⁴ A great number of studies have shown that NMA is an efficient and robust tool to determine the functionally conformational dynamics on the basis of protein static structures.^{25–27}

To make a systemic study of the molecular mechanism of protein conformational change and the effects from ligand binding, in the present study, we combine a normal-mode analysis (NMA) method in internal coordinates (iMOD)²⁵ and umbrella sampling MD simulation^{28,29} to investigate three typical protein systems: the phosphotransferase enzyme adenylate kinase (AdK, 214 amino acids (AA)) from *Escherichia coli*, the Ca²⁺-binding protein calmodulin (CaM, 148 AA), and the p38 α mitogen-activated protein kinase (MAPK, 354 AA). Normal mode analysis is used to find the dynamic pathway of the conformational transition between two given end points, and the umbrella sampling MD simulation is used to calculate the corresponding free-energy landscape. These proteins have different structural features, biological functions, and accordingly different conformational changes. The transition pathways of the conformational changes of these three proteins in the absence or presence of ligands are identified and energetically characterized. The captured transient structures along the minimum free-energy transition pathways of the three proteins and the calculated thermodynamic values are in good agreement with experimental data and results from other simulations, indicating the reliability of the present simulations in describing the thermodynamic properties of the conforma-

tional transitions of the proteins. The present simulation results show that AdK and CaM proteins are intrinsically flexible in structures with a wide ensemble of conformations sampled even in the absence of the respective ligands. The ligand binding modulates the free-energy landscape and switches the free-energy difference between the two end point structures for each protein. As a result, the conformational transitions of AdK and CaM are consistent with the “population shift” mechanism.^{4–6} In contrast, the conformational change of p38 α is a two-state transition, and the ligand binding leads to a large change in the free-energy barrier and thus promotes the transition from the DFG-in conformation to DFG-out conformation, likely following an “induced fit” conformational change mechanism.³ These observations indicate the mechanism diversity of protein conformational change, suggesting that the detailed mechanism of ligand binding and the associated conformational transition is not uniform for all kinds of proteins but may be correlated to their structural flexibility and respective biological functions.

THEORETICAL METHODS

Conformational Transition Pathway Generated by NMA. Normal mode analysis was performed using the iMOD program, with all heavy atoms of protein involved.²⁵ For AdK, the starting structure is the known crystal coordinate of the open state without bound inhibitor (PDB entry: 4AKE)³⁰ and the final target structure is from the close state bound with AP5A inhibitor (PDB entry: 1AKE).³¹ The starting and target structures of calmodulin are from coordinates of the NMR-measured calcium-free (1CFD)³² and crystal Ca²⁺-bound structures (1CLL).³³ And the starting and target structures of p38 α protein are from inhibitor-free DFG-in structure (1P38)³⁴ and pyridine 9 inhibitor bound DFG-out structure (1W83),³⁵ respectively. To investigate the effects of ligand binding to protein conformational transition, two sets of simulations (with or without ligand) were performed based on the experimentally measured conformations. Using AdK as an example, 4AKE and 1AKE with the removal of inhibitor were used as the end points to run NMA to generate the conformational transition pathway for ligand-free AdK. Meanwhile, 4AKE (the open state) with bound inhibitor was modified by positioning the AP5A inhibitor in the active site after superimposing heavy atoms in the open and closed forms. NMA was run again with the end points of 4AKE and 1AKE both bound with the inhibitor to generate the conformational transition pathway for ligand-bound AdK.

Multiple iterations of NMA were run to detect the transition pathway from the starting to final target structures gradually. In the iteration k , the intermediate structure $R^{(k)}$ is generated by the following equation:

$$R^{(k)} = R^{(k-1)} + v^{(k)} = R^{(k-1)} + S^{(k)} \sum_i^{m^{(k)}} (d^{(k-1)} \cdot u_i^{(k)}) u_i^{(k)} \quad (1)$$

where $R^{(k-1)}$ is the structure in iteration $(k-1)$ and $v^{(k)}$ is the combined displacement along $m^{(k)}$ low-frequency eigenmodes calculated by NMA. The displacement along the i th eigenmode is proportional to the projection $d^{(k-1)} \cdot u_i^{(k)}$ of the instantaneous distance vector $d^{(k-1)}$ on eigenvector $u_i^{(k)}$, and scaled by the step size $S^{(k)}$. The step size is used to control the iteration number and is set at 10.0 in this research. The number $m^{(k)}$ of modes at iteration k is determined by the following cumulative squared cosine function:

$$C(m^{(k)}) = \sum_i \cos^2(d^{(k-1)}, u_i^{(k)}) \quad (2)$$

The value of $m^{(k)}$ is the minimal number of modes which start from the low-frequency mode and end when $C(m^{(k)})$ reaches the cutoff value (0.8).^{26,36} The intermediate structure obtained in NMA calculation in each iteration was minimized with 1000 steps by molecular dynamics simulation, and the optimized structure was then used in next NMA iteration.

Umbrella Sampling Molecular Dynamics Simulation.

To compute the free-energy profile along the conformational transition pathway, umbrella sampling MD simulations were performed using the serial structures obtained from the above-mentioned NMA calculation as the starting points. In each umbrella sampling window, the sampling was performed with a biasing harmonic potential E_i on the ΔD_{rmsd} order parameter

$$E_i = k(\Delta D_{\text{rmsd}} - \Delta D_{\text{min},i})^2 \quad (3)$$

where k is the force constant; ΔD_{rmsd} is the order parameter which is defined as the difference in RMSD values of each structure from the reference starting and final states ($\Delta D_{\text{rmsd}} = \text{RMSD}(X_t, X_A) - \text{RMSD}(X_t, X_B)$, X_t is the instantaneous structure during simulation, and X_A and X_B are the two reference structures); and $\Delta D_{\text{min},i}$ is the value around which ΔD_{rmsd} is restrained.

A total of 45 windows for AdK, 47 windows for calmodulin, and 61 windows for p38 α were chosen from the NMA pathways with a step size of ~ 0.4 Å in the ΔD_{rmsd} space. The AMBER FF03 force field³⁷ and general Amber force field³⁸ were used to model proteins and ligands, respectively. The force field is well-developed and has been widely used in many simulations.^{39,40} As showed in Results, the thermodynamics parameters calculated using the force field are quite comparable to the experimental data and other MD simulations, suggesting that the dynamic motions of the proteins under study using the present force field are reasonable. In each window, the protein structure was solvated in a cubic TIP3P water box⁴¹ and neutralized by adding an appropriate number of counterions. The constructed system was then minimized for 5000 steps with the protein and/or ligand fixed using a harmonic restraint (using a force constant of $10 \text{ kcal mol}^{-1} \text{ \AA}^{-2}$ to apply to the heavy atoms). Subsequently, the system was heated from 0 to 300 K in 500 ps with a harmonic restraint (force constant = $10 \text{ kcal mol}^{-1} \text{ \AA}^{-2}$) applied to the heavy atoms. Finally, the equilibrium simulation (production run) for each window was performed using a weak ΔD_{rmsd} restraint of $10 \text{ kcal/mol/\AA}^2$ on protein heavy atoms (or the heavy atoms of the activation loop of p38 α kinase) for 2 ns.

The production run was performed at a constant temperature of 300 K and a constant pressure of 1 atm. The integration time step was set to 2 fs, and the temperature was regulated using Langevin dynamics with the collision frequency of 2 ps^{-1} . All the covalent bonds involving hydrogen atoms were fixed by the SHAKE algorithm.⁴² Periodic boundary conditions were used to avoid edge effects, and particle mesh Ewald method⁴³ was applied to treat the long-range electrostatic interaction. The cutoff distance for the long-range electrostatic and van der Waals energy terms was set to 10.0 Å. All simulations were carried out with the software AMBER10.⁴⁴

The last 1.5 ns simulation data of the production run in each window were collected, and the weighted histogram analysis

method (WHAM)²⁸ was used to calculate the potential of mean force (PMF) along the single ΔD_{rmsd} reaction coordinate. Using a protocol similar to that of Banavali et al.,¹⁸ the two-dimensional free-energy profile along ΔD_{rmsd} and other additional degrees of freedom was also calculated.

RESULTS

Structural Flexibility of LID Domain in Ligand-Free (apo) AdK. AdK is a monomeric phosphotransferase enzyme which catalyzes the phosphoryl transfer reaction ($\text{Mg}^{2+}\text{ATP} + \text{AMP} \leftrightarrow \text{Mg}^{2+}\text{ADP} + \text{ADP}$). An “open” conformation in the absence of the ligand and a “closed” conformation bound with a bisubstrate analog inhibitor AP₅A (a complex connecting ATP and AMP by a fifth phosphate, see Figure 1) were observed in

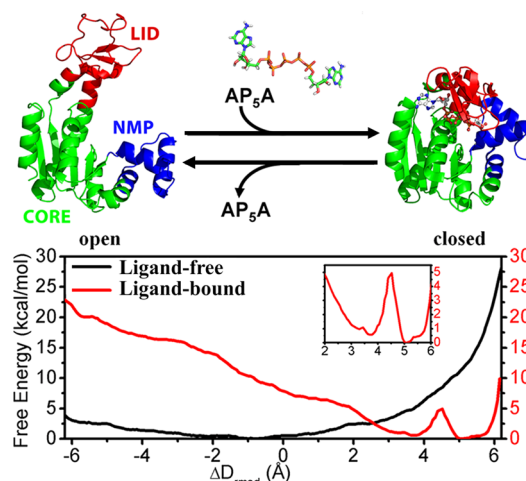


Figure 1. Top panel: crystallographic structures of open (4AKE) and closed (1AKE) states of AdK, along with the structure of AP₅A inhibitor. Bottom panel: one-dimensional free-energy profiles as a function of ΔD_{rmsd} for the conformational transitions of apo and ligand-bound AdK.

X-ray crystallography experiments.^{30,31} The conformational change between the two states is mainly focused on the two highly dynamic domains called LID (ATP binding domain of residues 118–167) and NMP (AMP binding domain of residues 30–67), whereas the CORE domain (residues 1–29, 68–117, and 161–214) is relatively rigid. Using the crystal open (4AKE)³⁰ and close (1AKE)³¹ structures as the end points, the free-energy landscape for the conformational transition of apo AdK was calculated along the reaction coordinate of the difference in root-mean-square deviation from the open to closed states of AdK (ΔD_{rmsd} , see the definition in Theoretical Methods). This reaction coordinate, ΔD_{rmsd} , can describe the position of the sampled conformations relative to both end point conformations at the same time and as a result has been often used in free-energy analysis for many biological systems.^{18,22,45} The choice of this reaction coordinate also allows a direct comparison of the present simulation results to those of other simulations. For instance, Figure S1 in the Supporting Information (SI) shows the one-dimensional free-energy profiles as a function of ΔD_{rmsd} for apo AdK in the present study and the comparison to that in the previous MD simulation by Arora et al.⁴⁵ The free-energy profiles share more or less the same shape, which to some extent indicates the reliability of the present simulation results.

As shown in Figure 1 (refer to the movie in Supporting Information for the conformational transition generated by NMA), the closed state ($\Delta D_{\text{rmsd}} = 6.5$ Å) has an energy much higher than that of the open state ($\Delta D_{\text{rmsd}} = -6.5$ Å) for apo AdK. In addition, a wide free-energy well is present in the range of ΔD_{rmsd} from -6.5 to ~ 1.0 Å without any observable energy barrier, corresponding to the experimentally observed flexibility of apo AdK within the range from the crystal open to closed structures.^{46,47} In this open free-energy well, the LID domain conformation could range from the open position to partially closed position, whereas the orientation of the NMP domain keeps relatively steady around its open state (see the representative structure of AdK with the lowest free energy in the free-energy well (-1.0 Å $\leq \Delta D_{\text{rmsd}} \leq 0.0$ Å) in Figure 2c). Therefore, the large-scale conformational change of AdK

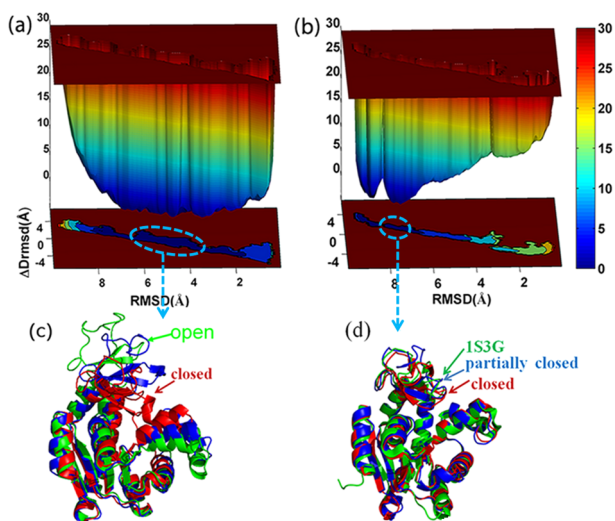


Figure 2. Two-dimensional free-energy landscapes for the conformational transitions of (a) apo and (b) ligand-bound AdK as a function of ΔD_{rmsd} and the RMSD value with respect to the crystal open state. (c) Comparison of the representative structure with the lowest free energy in the free-energy profile of apo AdK (blue) to the crystal open (green) and closed (red) structures. (d) Comparison of the representative partially closed structure of ligand-bound AdK (blue) to the crystal structure of the homologue enzyme from *Bacillus globisporus* (green, 1S3G) and the crystal closed structure of AdK (red).

from open to closed positions could easily start with the rapid shift of LID domain toward NMP (see the movie in Supporting Information). These structural characteristics are in agreement with the experimentally observed partially closed substates of apo AdK reported by Henzler-Wildman et al. (see Figure 2 in ref 47).

Another interesting observation for apo AdK is that the structure with the lowest free energy is not the open structure but the partially closed structure with its LID domain biased toward the closed position. This result is to some extent consistent with the observation in the fluorescence resonance energy transfer (FRET) experiment by Hanson et al.: the measurement of the distance between the dyes located in LID and CORE domains showed that the dynamic equilibrium of apo AdK favors the closed state of the LID domain.⁴⁶ Therefore, without the ligand, the LID domain may partially close, whereas closure of the NMP domain is less likely and requires the binding of the ligand (the energy of the closed

state is significantly higher than that of the open state for apo AdK; see Figure 1).

Ligand-Induced Biasing to Closed State of AdK. As shown in Figure 1, the binding of the AP₅A inhibitor significantly destabilizes the open state while stabilizing the closed state. The comparison of the free-energy landscape of apo AdK to that of inhibitor-bound AdK indicates an intersection region at around $\Delta D_{\text{rmsd}} = 2.6$ Å. This position could be considered as where the ligand-binding process occurs by drawing analogy between the binding process to the idea from the Marcus theory of electron transfer.^{45,48} Therefore, the ligand binding should occur concurrently with the conformational transition, which implies that the conformational transition of AdK might follow the “population shift” model: AdK could adopt various conformations, and the ligand binds selectively to some active conformation, causing the equilibrium to shift toward the ligand-bound conformation.^{4–6}

A small free-energy barrier is located at the position of $\Delta D_{\text{rmsd}} \approx 4.5$ Å which separates the fully closed state ($\Delta D_{\text{rmsd}} \geq 5$ Å) from a partially closed one ($\Delta D_{\text{rmsd}} \approx 3.7$ Å). This partially closed state in the presence of AP₅A inhibitor is different than the partially closed structure of apo AdK discussed earlier. The free-energy landscape as a function of ΔD_{rmsd} and the RMSD value with respect to the crystal open state is shown in Figure 2b to provide more detailed structural information for this partially closed state. The snapshots from the umbrella sampling MD simulation which satisfy the criteria of both 3.0 Å $< \Delta D_{\text{rmsd}} < 4.0$ Å and 6.0 Å $< \text{RMSD}_{\text{open}} < 8.0$ Å were chosen to be analyzed with hierarchical clustering, and the representative structure of the partially closed state is given in Figure 2d. This partially closed conformation differs from the fully closed conformation only in the LID domain which is slightly shifted to the open position in the former structure compared to the latter. Moreover, the same partially closed structure has been observed in the crystal structure of a homologue, an enzyme from *Bacillus globisporus* bound with the same inhibitor (PDB entry: 1S3G).⁴⁹ Therefore, the free-energy barrier at the position of $\Delta D_{\text{rmsd}} \approx 4.5$ Å corresponds to the opening and closing of the LID domain. Along the minimum free-energy pathway of the conformational transition from the open to closed states of ligand-bound AdK, the full closure of LID domain lags behind the closure of the NMP domain. In other words, it is the ligand binding that facilitates the accomplishment of the last stage of whole conformation change from open to closed state. A similar conclusion was reached in the free-energy calculations on AdK reported by Matsunaga et al.⁵⁰

Rate-Limiting Step of LID Domain Opening in the Catalytic Turnover. The dynamic NMR dispersion experiment by Wolf-Watz et al. measured the rates of opening and closing of nucleotide-binding lids (LID and NMP domains) during the catalytic turnover for AdK of both the mesophile *Escherichia coli* ($k_{\text{open}} = 286 \pm 85$ s^{−1}, $k_{\text{close}} = 1374 \pm 110$ s^{−1}, $k_{\text{cat}} = 263 \pm 30$ s^{−1}) and the hyperthermophile *Aquifex aeolicus* ($k_{\text{open}} = 44 \pm 20$ s^{−1}, $k_{\text{close}} = 1571 \pm 100$ s^{−1}, $k_{\text{cat}} = 30 \pm 10$ s^{−1}). The good correlation between the lid-opening rate and catalysis rate showed that the lid-opening motion is the rate-limiting step for the overall catalytic cycle.⁵¹ As shown in the inset PMF profile for the range 2.0 Å $\leq \Delta D_{\text{rmsd}} \leq 6.0$ Å in Figure 1, the observed partially closed state bound with AP₅A has a free energy higher than that of the fully closed state ($\Delta G \approx 0.62$ kcal/mol). The error bars calculated for the PMF (Figure S2 in Supporting Information) are very small in comparison with the

detailed free-energy values, indicating the small statistical uncertainty in the thermodynamics calculation. Therefore, the observed small free-energy difference should be not the lack of smoothness induced by insufficient sampling. The free-energy barrier corresponding to the opening of the LID domain is thus ~ 0.62 kcal/mol larger than that for the closing of LID, specifically identifying the key rate-limiting step of LID domain opening when bound to a ligand, consistent with multiple previous studies.^{52,53} Using this free-energy barrier difference, the closing rate of LID can be evaluated to be 2.85 times larger than the opening rate ($k_{\text{close}}/k_{\text{open}} \propto \exp((\Delta G_{\text{open}}^* - \Delta G_{\text{close}}^*)/k_{\text{B}}T)$), which is close to the experimentally measured ratio between the lid-closing and lid-opening rates ($k_{\text{close}}/k_{\text{open}} = 4.80$).⁵¹

Inherent Structural Flexibility of Both apo and Ca^{2+} -Bound Calmodulin. CaM is involved in the regulation of a variety of cellular signaling pathways.^{54,55} The apo CaM adopts a “closed” conformation in which the helix–loop–helix motifs in both N- and C-domains are packed tightly together. The binding of four Ca^{2+} ions to the helix–loop–helix motifs leads to a large-scale conformational change and an “open” conformation (see Figure 3 and the movie in Supporting Information) in which the hydrophobic binding pocket of each helix–loop–helix motif is exposed and can be used to bind to various target proteins.^{32,33}

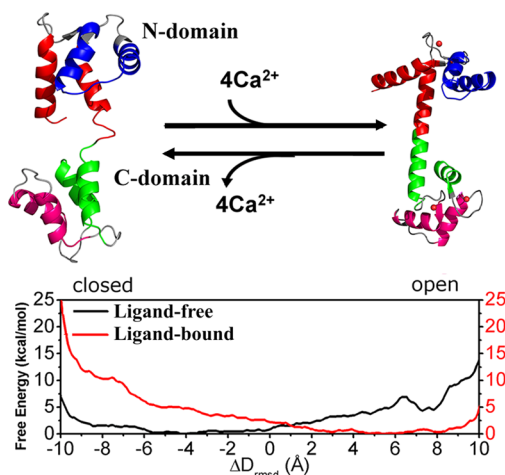


Figure 3. Top panel: crystallographic structure of open state (1CLL) and NMR-measured structure of closed state (1CFD) of calmodulin. Bottom panel: one-dimensional free-energy profiles as a function of ΔD_{rmsd} for the conformational transitions of apo and Ca^{2+} -bound calmodulin.

As shown in Figure 3, wide free-energy wells are present in the free-energy profiles for the conformational transitions of both apo and Ca^{2+} -bound CaM. The range in which the free energy is lower than 5 kcal/mol spans from -10.0 Å (closed state) to 6.0 Å for apo CaM and from -5.0 Å to 10.0 Å (open state) for Ca^{2+} -bound CaM, strongly suggesting that the structure of CaM is flexible with or without bound Ca^{2+} ions. In addition, the conformations adopted by CaM are biased to the closed state in the absence of Ca^{2+} ions, whereas the binding of Ca^{2+} promotes the conformational change toward the open state. CaM and its individual domains have consistently been shown to be highly dynamic and flexible in a great number of experiments and theoretical simulations.^{56–59}

In this study the structure with the lowest free energy is neither the crystal closed nor the open structure in both free-energy landscapes. The representative structure of Ca^{2+} -bound CaM with the lowest free energy in the free-energy well (5.0 Å $\leq \Delta D_{\text{rmsd}} \leq 8.0$ Å) is very similar to the crystal open structure with small differences only in N- and C-domains (Figure 4). The orientations of helices V and VIII in the C-domain slightly deviate from the analogues in the crystal open structure, whereas the orientations of helices I and IV in the N-domain show more extreme deviation, indicating that the N-domain in the stable structure of Ca^{2+} -bound CaM is less open than the C-domain (Figure 4b). The same phenomenon was observed by several earlier NMR experiments.^{60,61} In contrast to Ca^{2+} -bound CaM, of the representative structures with the lowest free energy in the free-energy well (-6.0 Å $\leq \Delta D_{\text{rmsd}} \leq -4.0$ Å) of apo CaM, the helices V and VIII in the C-domain show deviations from their closed positions that are larger than those of helices I and IV in the N-domain (Figure 4a). This observation suggests that the C-domain is less stable than the N-domain in the absence of Ca^{2+} , again consistent with the observations in multiple experiments.^{62,63}

An extensive survey for the homologues of calmodulin with at least 90% sequence identity was performed in the Protein Data Bank (PDB) to show the structural diversity of CaM in apo and Ca^{2+} -bound states. Excluding those structures bound with other protein or peptides, these experimental structures (either apo or Ca^{2+} -bound) can be found in the corresponding transition pathway of apo or Ca^{2+} -bound CaM in the two-dimensional free-energy landscape as a function of ΔD_{rmsd} and RMSD with respect to the closed state (Figure 5). The NMR structures (PDB entries 1CFD and 1DMO for apo CaM and 1X02 for Ca^{2+} -bound CaM) are found distributed unevenly along the corresponding transition pathway. Impressively, 1CFD and 1DMO are biased to the closed state whereas 1X02 is biased to the open state. The X-ray structures of 1Y6W, 2YGG, and 1UP5 with calcium bound are located at around $\Delta D_{\text{rmsd}} = 8\text{--}10$ Å, very close to the open state of Ca^{2+} -bound CaM. Hence, X-ray crystallography is propitious for determining energetically stable structures while NMR is favorable for sampling a variety of conformations around low-energy structures. All these observations indicate that the method used here is able to capture the transient structures along the pathway of the conformational transition of calmodulin. Both apo and Ca^{2+} -bound calmodulins display high levels of flexibility, which suggests that the conformational change of this protein might also follow the “population shift” mechanism. It should be pointed out that some of the NMR structures deviate from the conformations on the pathway between the closed and open states, which might be the conformations the other target proteins bind with.

Two-State Transition between DFG-in and DFG-out Conformations of p38 α Kinase and the Effect of Inhibitor Binding on the Free-Energy Barrier. P38 α kinase plays an important role in cellular responses to external stress, and the inhibitors of p38 α have been shown to have anti-inflammatory effects in preclinical disease models.⁶⁴ In contrast to AdK and CaM, the conformational change in p38 α kinase is focused on the activation loop which contains a largely conserved DFG (Asp168-Phe169-Gly170) motif in the kinase protein superfamily. The DFG motif within the activation loop is able to switch between the “DFG-in” (catalytically active) and “DFG-out” (catalytically inactive) states, controlling the functional status of the protein (see Figure 6 and the movie in

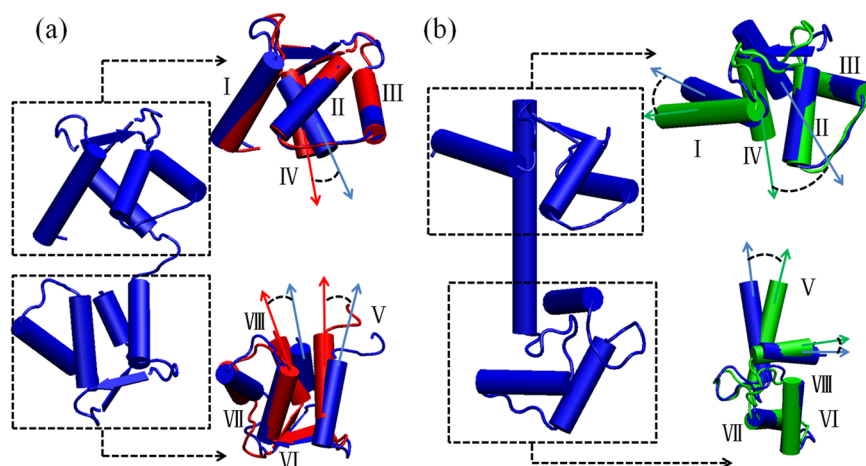


Figure 4. (a) Cartoon diagram of the representative structure with the lowest free energy for apo CaM (blue) and the comparison of N- and C-domains to those in the NMR measured closed structure (red). (b) Cartoon diagram of the representative structure with the lowest free energy for Ca^{2+} -bound CaM (blue) and comparison of N- and C-domains to those in the crystal open structure (green). To see the N-domain difference in these structures, the structures are overlaid such that the fit between helices II and III (residues of 29–54) within the helix–loop–helix motif in the N-domain is optimized. For the C-domain comparison, the structure superposition is optimized for helices VI and VII (residues of 102–127). The orientations of the remaining helices are shown by arrows.

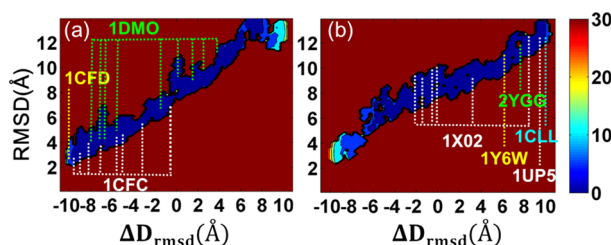


Figure 5. The two-dimensional free-energy landscapes for the conformational transitions of (a) apo and (b) Ca^{2+} -bound calmodulin as a function of ΔD_{rmsd} and the RMSD value with respect to the closed state.

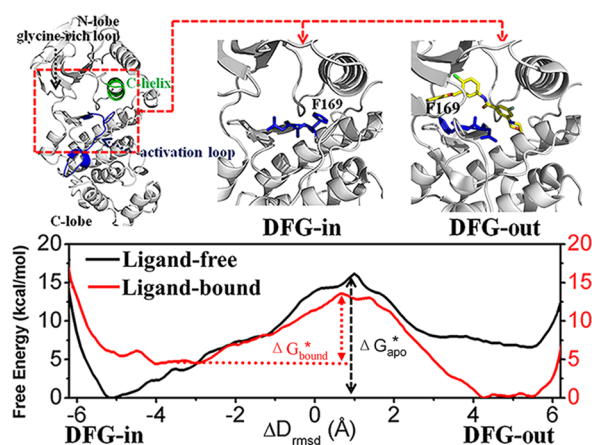


Figure 6. Top panel: crystallographic structure of p38 α kinase with a detailed view of the DFG motif in the DFG-in (1P38) and DFG-out (1W83) conformations. Bottom panel: one-dimensional free-energy profiles as a function of ΔD_{rmsd} for the conformational transitions of apo and ligand-bound p38 α kinase.

Supporting Information).^{34,35} Figure 6 shows the free-energy landscape as a function of ΔD_{rmsd} within the region of the activation loop (Asp168–Glu178). The presence of two minima corresponding to the DFG-in and DFG-out states and the large free-energy barrier separating them make the free-energy

landscape of p38 α significantly different from those of AdK and CaM. In the absence of an inhibitor, the DFG-in state is ~ 7.0 kcal/mol more stable than the DFG-out state and the activation free energy (the free-energy barrier from DFG-in state to DFG-out state, ΔG_{apo}^* in Figure 6) is 16.4 kcal/mol. The DFG-in conformation is therefore thermodynamically favored in apo p38 α , which is consistent with the experimental observations that the DFG-in conformation can be steadily sampled both free and in complex with inhibitor whereas the DFG-out conformation can be sampled only infrequently in the presence of specific inhibitors.^{65–67}

The free-energy difference between DFG-in and DFG-out states is very similar to that measured in the MD simulations for other protein kinases, e.g., the measured free-energy difference of 4.0 ± 0.5 kcal/mol for c-Src and 6.0 ± 0.5 kcal/mol for c-Abl kinases with the binding of imatinib inhibitor⁶⁸ and 4–6 kcal/mol for apo cyclin-dependent kinase (CDK5).⁶⁹ In addition, the measured activation free energy (from DFG-in to DFG-out state) is also similar to previous simulation results: the activation free energy was predicted to be ~ 16 –20 kcal/mol for apo CDK5⁶⁹ and ~ 20 kcal/mol for c-Src kinase.⁷⁰

The binding of pyridine 9 inhibitor decreases the DFG-in to DFG-out activation free energy (9.0 kcal/mol ($\Delta G_{\text{bound}}^*$ in Figure 6), which is 7.4 kcal/mol less than that for apo p38 α), promoting the transition from DFG-in to DFG-out and stabilizing the latter state (the free energy of the DFG-in state becomes ~ 4.8 kcal/mol higher than that of the DFG-out state). Figure 7a,b shows the two-dimensional free-energy landscapes as a function of ΔD_{rmsd} and the RMSD with respect to the DFG-in crystal structures for apo and inhibitor-bound p38 α , with transition states present for $0.0 \text{ \AA} < \Delta D_{\text{rmsd}} < 2.0 \text{ \AA}$ and $5.0 \text{ \AA} < \text{RMSD}_{\text{DFG-in}} < 7.0 \text{ \AA}$. In the representative structure of the transition state for apo p38 α (Figure 7c), the side chain of F169 is located midway between the DFG-in and DFG-out positions. The details of the interactions between the DFG motif and the surrounding residues can be seen in the side view with a 90° rotation (Figure 7d): the side chain of F169 forms a cation– π interaction with K53 and the side-chain carboxylate oxygen of D168 forms a hydrogen bond with the side-chain amide of N154.

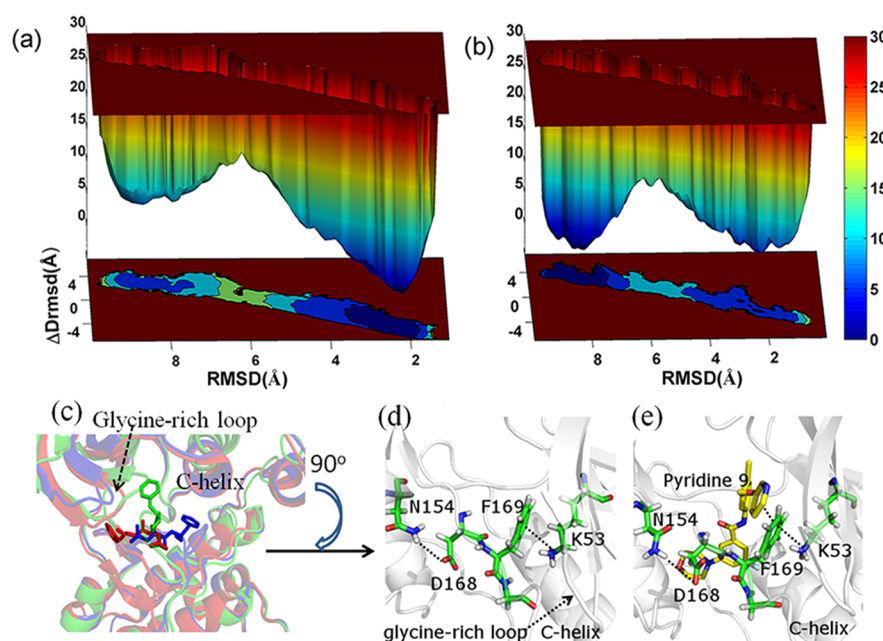


Figure 7. Two-dimensional free-energy landscapes for the conformational transitions of (a) apo and (b) ligand-bound p38 α kinase as a function of ΔD_{rmsd} and the RMSD value with respect to the DFG-in state. (c) Comparison of the representative structure of the transition state (green) to the DFG-in (blue) and DFG-out (red) conformations. Detailed interactions between DFG motif and the surrounding residues or inhibitor in the transition states of (d) apo and (e) ligand-bound p38 α kinase.

The same interactions can also be seen in the transition state of inhibitor-bound p38 α (Figure 7e). Moreover, the pyridine 9 inhibitor also has a π – π interaction with F169 and thus further stabilizes the transition state. The cation– π interaction formation between F169 and K53 was also observed in the intermediate conformations of p38 α in an accelerated MD simulation reported by Filomia et al.⁷¹ These results suggest that the pyridine 9 inhibitor is able to bind not only to the DFG-out state but also to the DFG-in state. Both states have relatively low free energy, and pyridine 9 binding changes the free-energy difference of the two states, decreases the activation free energy, and promotes the DFG-in to DFG-out transition. Combined with the experimental observation that the DFG-in structure can be measured for both apo and inhibitor-bound p38 α whereas the DFG-out structure has been captured only in the presence of specific inhibitors, the present simulation results suggest that the conformational transition of p38 α may follow the “induced fit” mechanism.³

Effect of Protonation of D168 on the Free-Energy Barrier. It has been proposed in the MD simulation study by Shan et al. that the protonation of D404 within the DFG motif of Abl kinase plays an important role in controlling the DFG flip.⁷² Moreover, the free-energy calculation in the MD simulation by Lovera et al. indicated that the D404 protonation in c-Abl kinase leads to the stabilization of DFG-out state by 1.4 ± 0.9 kcal/mol.⁶⁸ In contrast, the D404 protonation in c-Src kinase makes the DFG-out state less favorable by 2.0 ± 0.9 kcal/mol.⁶⁸ By calculating the pK_a value of D404 (4.0 ± 0.5 in DFG-in and 2.6 ± 0.3 in DFG-out state), the authors suggested that the aspartate protonation might be improbable in DFG-out state of c-Src kinase.⁶⁸ In the present study, we also addressed the influence of the aspartate protonation on the free-energy landscape of the conformational transition of p38 α . As shown in Figure 8, the protonation of D168 reduces the free-energy difference between the DFG-in and DFG-out states by 1.94 kcal/mol for apo and 1.59 kcal/mol for ligand-bound p38 α ,

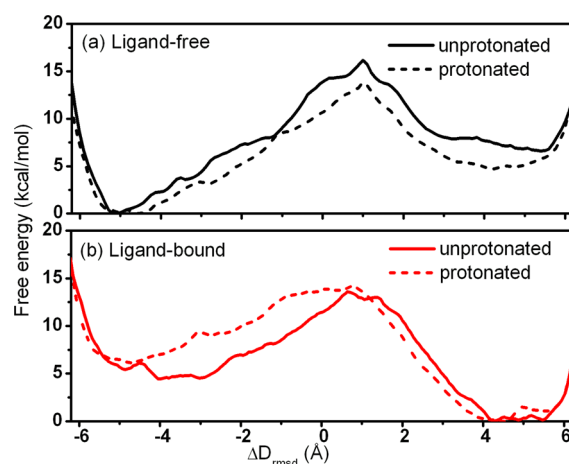


Figure 8. The one-dimensional free-energy profiles as a function of ΔD_{rmsd} for the conformational transitions of (a) apo and (b) ligand-bound p38 α kinase (solid line, unprotonated kinase; dashed line, protonated kinase).

respectively. The detailed analysis shows that the proton in the side chain of D168 forms an additional hydrogen bond with the side-chain carboxylate oxygen of the neighboring E150 and thus further stabilizes the DFG-out state. These numbers are very close to the free-energy differences induced by aspartate protonation for c-Abl and c-Src kinases.⁶⁸ Moreover, the reduced free-energy difference between the two functional states of p38 α by aspartate protonation (by stabilizing DFG-out state relative to DFG-in state) is supposed to facilitate the conformational interconversion, which is certainly consistent with the observation of Shan et al.⁷²

DISCUSSION

The protein conformational transition coupled with the biological function has attracted much attention in the last

several decades. Various methods in both experiments and theoretical simulations have been utilized to understand the molecular mechanism of protein conformational transition. However, the difficulty in capturing the transition pathway makes the mechanism unclear yet. The crucial question remains what is the correlation between the protein conformational transition and the ligand binding? The induced fit and population shift models have been proposed to answer this question. The former model suggested that the protein conformational transition is solely induced by the binding of the ligand,³ whereas the latter model proposed that the protein itself is in a dynamic equilibrium between the functional structures and the ligand binds selectively to an active conformation and forces the equilibrium to the ligand-bound structure.^{4–6}

In the present study, to understand which model best describes the ligand-free and ligand-bound protein conformational transitions, various conformational transitions of protein systems including AdK, p38 α kinases, and calmodulin in the absence and presence of respective ligands are investigated using the combination of NMA and umbrella sampling molecular dynamics. NMA has been widely used in the theoretical studies on the conformational dynamics of various proteins. Despite the great success of NMA, discrepancy exists between the amplitude of thermal fluctuations of harmonic oscillators described by normal modes and the amplitude of protein conformational transition: NMA is based on a harmonic approximation of the dynamics of a system about local energy minima, whereas the large-scale conformational dynamics of proteins are presumably highly anharmonic because of the rugged energy landscape and severe solvent damping.^{73,74} To investigate the anharmonic aspects of protein dynamics, Levy et al. developed quasiharmonic analysis based on the principal component analysis of molecular dynamics trajectory, which generates quasiharmonic modes comparable to the normal modes from NMA.⁷⁵ Hayward et al. used quasiharmonic analysis on the simulation of an isolated bovine pancreatic trypsin inhibitor and indicated that the inaccurate description of anharmonic atomic fluctuations in protein by NMA only leads to the underestimation of the mean-squared fluctuation of atomic coordinates along the direction of the eigenvector.^{76,77} Nevertheless, the eigenvectors of the lowest modes generated by NMA constitute an essential subspace of the collective coordinates and thus gives good description of collective motions in proteins.^{78,79} Therefore, it is believed that the directions but not the magnitudes of the collective motions captured by the eigenvectors of the lowest modes of NMA are insensitive to the details of microscopic interactions and solvent damping.^{24,80} As a result, without considering the anharmonic effects, NMA could still provide the detailed pathway of protein conformational transition. In the present study, the intermediate structures of protein conformational transition are calculated by the iterative process as shown in eq 1. Each intermediate structure is obtained from the combined displacement along multiple functional lowest-frequency modes of NMA. The direction of the displacement is determined by the instantaneous distance vector on eigenvector and the magnitude is controlled by the step size defined in eq 1. Multiple values of the step size were tested in the simulation for each protein under study, which generate a consistent transition pathway consisting of different numbers of middle points, indicating the robustness and efficiency of the NMA method

used here in measuring the transition pathway of protein conformational change.

The accuracy of the present study in describing protein motions is evaluated by comparing the simulation results to many sets of experimental data and other simulation results. The inherent structural flexibility of AdK and calmodulin and the measured transient structures along the minimum free-energy transition pathways of both proteins in the absence and presence of ligands are in agreement with the experimental data.^{46,47,51,81} The calculated activation free energy of p38 α is very similar to those of other MAPK proteins such as CDK5,⁶⁹ c-Src,⁷⁰ and c-Abl kinases.⁶⁸ Therefore, the transition pathways for the proteins under study are not simple connections between end point structures but do reflect the real dynamic motions of proteins e.g., the cooperative motions of domains in AdK and CaM (see the movies in Supporting Information).

On the basis of the simulation results consistent with the previous experimental data and other simulation results, the present study predicts that the ligand binding could play different roles for different kinds of conformational transitions. For the inherently flexible proteins like AdK and calmodulin, the ligands may not bind to the corresponding apo-like conformations directly but to some intermediate conformations and assist in completing the conformational transitions. Thus, the ligand binding and conformational transition of the two proteins should follow the “population shift” mechanism. On the other hand, for p38 α kinase, the conformational change which is focused on local activation of the loop responsible for the opening and closing of the binding cavity, the inhibitor binds to the apo-like conformation directly and promotes the conversion from the catalytically active DFG-in conformation to catalytically inactive DFG-out conformation. As a result, the conformational transition of p38 α kinase likely follows the “induced fit” mechanism. Therefore, both population shift and induced fit models exist among protein conformational transition. Which model a protein adopts for its conformational transition should be correlated to the biological function of the protein.

■ ASSOCIATED CONTENT

● Supporting Information

Figures with the comparison of the free-energy profile of apo Adk in the present study to that in the previous MD simulation by Arora et al.⁴⁵ and the error bar calculated for the free-energy profile of ligand-bound AdK; movies generated by normal-mode analysis that show the conformational transitions of the three proteins under study. This material is available free of charge via the Internet at <http://pubs.acs.org>.

■ AUTHOR INFORMATION

Corresponding Authors

*Q.S.: tel, +86 21 50806600-1304; e-mail, qshao@mail.shcnc.ac.cn.

*J.S.: tel, +1 919 767 2555; e-mail, Jiye.Shi@ucb.com.

*W.Z.: tel, +86 21 50805020; e-mail, wzhu@mail.shcnc.ac.cn.

Notes

The authors declare no competing financial interest.

■ ACKNOWLEDGMENTS

We thank the National 863 Program (Grant 2012AA01A305), National Natural Science Foundation of China (NNSFC) (Grants 21373258, 21021063, and 81273435) and the National

Basic Research Program of China (973) (Grant 2012CB910403) for financial support. The simulations were run at Shanghai Supercomputing Center (SSC) and TianHe 1 supercomputer in Tianjian. We acknowledge Mr. Xiuming Xiong for the help in preparing the movies.

REFERENCES

- (1) Bakan, A.; Bahar, I. The Intrinsic Dynamics of Enzymes Plays a Dominant Role in Determining the Structural Changes Induced upon Inhibitor Binding. *Proc. Natl. Acad. Sci. U.S.A.* **2009**, *106*, 14349–14354.
- (2) Grant, B. J.; Gofre, A. A.; McCammon, J. A. Large Conformational Changes in Proteins: Signaling and Other Functions. *Curr. Opin. Struct. Biol.* **2010**, *20*, 142–147.
- (3) Koshland, D. E. Application of a Theory of Enzyme Specificity to Protein Synthesis. *Proc. Natl. Acad. Sci. U.S.A.* **1958**, *44*, 98–104.
- (4) Tsai, C. J.; Ma, B. Y.; Nussinov, R. Folding and Binding Cascades: Shifts in Energy Landscapes. *Proc. Natl. Acad. Sci. U.S.A.* **1999**, *96*, 9970–9972.
- (5) Volkman, B. F.; Lipson, D.; Wemmer, D. E.; Kern, D. Two-State Allosteric Behavior in a Single Domain Signaling Protein. *Science* **2001**, *291*, 2429–2433.
- (6) Boehr, D. D.; Nussinov, R.; Wright, P. E. The Role of Dynamic Conformational Ensembles in Biomolecular Recognition. *Nat. Chem. Biol.* **2009**, *5*, 789–796.
- (7) Kokkinidis, M.; Glykos, N. M.; Fadoulglou, V. E. Protein Flexibility and Enzymatic Catalysis. *Adv. Protein Chem. Struct. Biol.* **2012**, *87*, 181–218.
- (8) Westenhoff, S.; Nazarenko, E.; Malmerberg, E.; Davidsson, J.; Katona, G.; Neutze, R. Time-Resolved Structural Studies of Protein Reaction Dynamics: A Smorgasbord of X-Ray Approaches. *Acta Crystallogr., Sect. A* **2010**, *66*, 207–219.
- (9) Dror, R. O.; Dirks, R. M.; Grossman, J. P.; Xu, H. F.; Shaw, D. E. Biomolecular Simulation: A Computational Microscope for Molecular Biology. *Annu. Rev. Biophys.* **2012**, *41*, 429–452.
- (10) Skjaerven, L.; Reuter, N.; Martinez, A. Dynamics, Flexibility and Ligand-Induced Conformational Changes in Biological Macromolecules: A Computational Approach. *Future Med. Chem.* **2011**, *3*, 2079–2100.
- (11) Karplus, M.; McCammon, J. A. Molecular Dynamics Simulations of Biomolecules. *Nat. Struct. Biol.* **2002**, *9*, 646–652.
- (12) Hansson, T.; Oostenbrink, C.; van Gunsteren, W. Molecular Dynamics Simulations. *Curr. Opin. Struct. Biol.* **2002**, *12*, 190–196.
- (13) Klepeis, J. L.; Lindorff-Larsen, K.; Dror, R. O.; Shaw, D. E. Long-Timescale Molecular Dynamics Simulations of Protein Structure and Function. *Curr. Opin. Struct. Biol.* **2009**, *19*, 120–127.
- (14) Schlitter, J.; Engels, M.; Kruger, P. Targeted Molecular Dynamics: A New Approach for Searching Pathways of Conformational Transitions. *J. Mol. Graphics* **1994**, *12*, 84–89.
- (15) Hamelberg, D.; Mongan, J.; McCammon, J. A. Accelerated Molecular Dynamics: A Promising and Efficient Simulation Method for Biomolecules. *J. Chem. Phys.* **2004**, *120*, 11919–11929.
- (16) Bussi, G.; Laio, A.; Parrinello, M. Equilibrium Free Energies from Nonequilibrium Metadynamics. *Phys. Rev. Lett.* **2006**, *96*, 090601.
- (17) Hansmann, U. H. E. Parallel Tempering Algorithm for Conformational Studies of Biological Molecules. *Chem. Phys. Lett.* **1997**, *281*, 140–150.
- (18) Banavali, N. K.; Roux, B. Free Energy Landscape of A-DNA to B-DNA Conversion in Aqueous Solution. *J. Am. Chem. Soc.* **2005**, *127*, 6866–6876.
- (19) Berteotti, A.; Cavalli, A.; Branduardi, D.; Gervasio, F. L.; Recanatini, M.; Parrinello, M. Protein Conformational Transitions: The Closure Mechanism of a Kinase Explored by Atomistic Simulations. *J. Am. Chem. Soc.* **2008**, *131*, 244–250.
- (20) Fornili, A.; Giabbai, B.; Garau, G.; Degano, M. Energy Landscapes Associated with Macromolecular Conformational Changes from Endpoint Structures. *J. Am. Chem. Soc.* **2010**, *132*, 17570–17577.
- (21) Elber, R. Simulations of Allosteric Transitions. *Curr. Opin. Struct. Biol.* **2011**, *21*, 167–172.
- (22) Yu, H. B.; Ma, L.; Yang, Y.; Cui, Q. Mechanochemical Coupling in the Myosin Motor Domain. I. Insights from Equilibrium Active-Site Simulations. *PLoS Comput. Biol.* **2007**, *3*, 199–213.
- (23) Golosov, A. A.; Warren, J. J.; Beese, L. S.; Karplus, M. The Mechanism of the Translocation Step in DNA Replication by DNA Polymerase I: A Computer Simulation Analysis. *Structure* **2010**, *18*, 83–93.
- (24) Ma, J. P. Usefulness and Limitations of Normal Mode Analysis in Modeling Dynamics of Biomolecular Complexes. *Structure* **2005**, *13*, 373–380.
- (25) Lopez-Blanco, J. R.; Garzon, J. I.; Chacon, P. iMod: Multipurpose Normal Mode Analysis in Internal Coordinates. *Bioinformatics* **2011**, *27*, 2843–2850.
- (26) Yang, Z.; Majek, P.; Bahar, I. Allosteric Transitions of Supramolecular Systems Explored by Network Models: Application to Chaperonin GroEL. *PLoS Comput. Biol.* **2009**, *5*, e1000360.
- (27) Cui, Q.; Li, G.; Ma, J.; Karplus, M. A Normal Mode Analysis of Structural Plasticity in the Biomolecular Motor F₁-ATPase. *J. Mol. Biol.* **2004**, *340*, 345–372.
- (28) Kumar, S.; Bouzida, D.; Swendsen, R. H.; Kollman, P. A.; Rosenberg, J. M. The Weighted Histogram Analysis Method for Free-Energy Calculations on Biomolecules 0.1. The Method. *J. Comput. Chem.* **1992**, *13*, 1011–1021.
- (29) Kumar, S.; Rosenberg, J. M.; Bouzida, D.; Swendsen, R. H.; Kollman, P. A. Multidimensional Free-Energy Calculations Using the Weighted Histogram Analysis Method. *J. Comput. Chem.* **1995**, *16*, 1339–1350.
- (30) Müller, C.; Schlauderer, G.; Reinstein, J.; Schulz, G. Adenylate Kinase Motions during Catalysis: An Energetic Counterweight Balancing Substrate Binding. *Structure* **1996**, *4*, 147–156.
- (31) Müller, C. W.; Schulz, G. E. Structure of the Complex between Adenylate Kinase from *Escherichia coli* and the Inhibitor Ap₅A Refined at 1.9 Å Resolution: A Model for a Catalytic Transition State. *J. Mol. Biol.* **1992**, *224*, 159–177.
- (32) Kuboniwa, H.; Tjandra, N.; Grzesiek, S.; Ren, H.; Klee, C. B.; Bax, A. Solution Structure of Calcium-Free Calmodulin. *Nat. Struct. Biol.* **1995**, *2*, 768–776.
- (33) Chattopadhyaya, R.; Meador, W. E.; Means, A. R.; Quirocho, F. A. Calmodulin Structure Refined at 1.7 Å Resolution. *J. Mol. Biol.* **1992**, *228*, 1177–1192.
- (34) Wang, Z.; Harkins, P. C.; Ulevitch, R. J.; Han, J.; Cobb, M. H.; Goldsmith, E. J. The Structure of Mitogen-Activated Protein Kinase P38 at 2.1-Å Resolution. *Proc. Natl. Acad. Sci. U.S.A.* **1997**, *94*, 2327–2332.
- (35) Gill, A. L.; Frederickson, M.; Cleasby, A.; Woodhead, S. J.; Carr, M. G.; Woodhead, A. J.; Walker, M. T.; Congreve, M. S.; Devine, L. A.; Tisi, D.; et al. Identification of Novel p38α MAP Kinase Inhibitors Using Fragment-Based Lead Generation. *J. Med. Chem.* **2005**, *48*, 414–426.
- (36) Marques, O.; Sanejouand, Y. H. Hinge-Bending Motion in Citrate Synthase Arising from Normal Mode Calculations. *Proteins* **1995**, *23*, 557–560.
- (37) Duan, Y.; Wu, C.; Chowdhury, S.; Lee, M. C.; Xiong, G.; Zhang, W.; Yang, R.; Cieplak, P.; Luo, R.; Lee, T.; et al. A Point-Charge Force Field for Molecular Mechanics Simulations of Proteins Based on Condensed-Phase Quantum Mechanical Calculations. *J. Comput. Chem.* **2003**, *24*, 1999–2012.
- (38) Wang, J.; Wolf, R. M.; Caldwell, J. W.; Kollman, P. A.; Case, D. A. Development and Testing of a General Amber Force Field. *J. Comput. Chem.* **2004**, *25*, 1157–1174.
- (39) Kondo, H. X.; Okimoto, N.; Morimoto, G.; Taiji, M. Free-Energy Landscapes of Protein Domain Movements upon Ligand Binding. *J. Phys. Chem. B* **2011**, *115*, 7629–7636.
- (40) Cui, W.; Cheng, Y.-H.; Geng, L.-L.; Liang, D.-S.; Hou, T.-J.; Ji, M.-J. Unraveling the Allosteric Inhibition Mechanism of PTP1B by Free Energy Calculation Based on Umbrella Sampling. *J. Chem. Inf. Model.* **2013**, *53*, 1157–1167.

- (41) Jorgensen, W. L.; Chandrasekhar, J.; Madura, J. D.; Impey, R. W.; Klein, M. L. Comparison of Simple Potential Functions for Simulating Liquid Water. *J. Chem. Phys.* **1983**, *79*, 926–935.
- (42) Ryckaert, J.-P.; Ciccotti, G.; Berendsen, H. J. Numerical Integration of the Cartesian Equations of Motion of a System with Constraints: Molecular Dynamics of *n*-Alkanes. *J. Chem. Phys.* **1977**, *23*, 327–341.
- (43) Darden, T.; York, D.; Pedersen, L. Particle Mesh Ewald: An $N \log(N)$ Method for Ewald Sums in Large Systems. *J. Chem. Phys.* **1993**, *98*, 10089.
- (44) Case, D. A.; Darden, T. A.; Cheatham, T. E., III; Simmerling, C. L.; Wang, J.; Duke, R. E.; Luo, R.; Crowley, M.; Walker, R. C.; Zhang, W.; et al. AMBER10; University of California: San Francisco, 2008.
- (45) Arora, K.; Brooks, C. L. Large-Scale Allosteric Conformational Transitions of Adenylate Kinase Appear to Involve a Population-Shift Mechanism. *Proc. Natl. Acad. Sci. U.S.A.* **2007**, *104*, 18496–18501.
- (46) Hanson, J. A.; Duderstadt, K.; Watkins, L. P.; Bhattacharyya, S.; Brokaw, J.; Chu, J.-W.; Yang, H. Illuminating the Mechanistic Roles of Enzyme Conformational Dynamics. *Proc. Natl. Acad. Sci. U.S.A.* **2007**, *104*, 18055–18060.
- (47) Henzler-Wildman, K. A.; Thai, V.; Lei, M.; Ott, M.; Wolf-Watz, M.; Fenn, T. Intrinsic Motions along an Enzymatic Reaction Trajectory. *Nature* **2007**, *450*, 838–844.
- (48) Marcus, R. A.; Sutin, N. Electron Transfers in Chemistry and Biology. *Biochim. Biophys. Acta* **1985**, *811*, 265–322.
- (49) Bae, E.; Phillips, G. N. Structures and Analysis of Highly Homologous Psychrophilic, Mesophilic, and Thermophilic Adenylate Kinases. *J. Biol. Chem.* **2004**, *279*, 28202–28208.
- (50) Matsunaga, Y.; Fujisaki, H.; Terada, T.; Furuta, T.; Moritsugu, K.; Kidera, A. Minimum Free Energy Path of Ligand-Induced Transition in Adenylate Kinase. *PLoS Comput. Biol.* **2012**, *8*, e1002555.
- (51) Wolf-Watz, M.; Thai, V.; Henzler-Wildman, K.; Hadjipavlou, G.; Eisenmesser, E. Z.; Kern, D. Linkage between Dynamics and Catalysis in a Thermophilic-Mesophilic Enzyme Pair. *Nat. Struct. Mol. Biol.* **2004**, *11*, 945–949.
- (52) Whitford, P. C.; Miyashita, O.; Levy, Y.; Onuchic, J. N. Conformational Transitions of Adenylate Kinase: Switching by Cracking. *J. Mol. Biol.* **2007**, *366*, 1661–1671.
- (53) Adkar, B. V.; Jana, B.; Bagchi, B. Role of Water in the Enzymatic Catalysis: Study of $\text{ATP} + \text{AMP} \rightarrow 2\text{ADP}$ Conversion by Adenylate Kinase. *J. Phys. Chem. A* **2011**, *115*, 3691–3697.
- (54) Chin, D.; Means, A. R. Calmodulin: A Prototypical Calcium Sensor. *Trends Cell Biol.* **2000**, *10*, 322–328.
- (55) Grabarek, Z. Structure of a Trapped Intermediate of Calmodulin: Calcium Regulation of EF-hand Proteins from a New Perspective. *J. Mol. Biol.* **2005**, *346*, 1351–1366.
- (56) Chen, B. W.; Lowry, D. F.; Mayer, M. U.; Squier, T. C. Helix A Stabilization Precedes Amino-terminal Lobe Activation upon Calcium Binding to Calmodulin. *Biochemistry* **2008**, *47*, 9220–9226.
- (57) Gsponer, J.; Christodoulou, J.; Cavalli, A.; Bui, J. M.; Richter, B.; Dobson, C. M.; Vendruscolo, M. A Coupled Equilibrium Shift Mechanism in Calmodulin-Mediated Signal Transduction. *Structure* **2008**, *16*, 736–746.
- (58) Zhang, M.; Abrams, C.; Wang, L. P.; Gizzi, A.; He, L. P.; Lin, R. H.; Chen, Y.; Loll, P. J.; Pascal, J. M.; Zhang, J. F. Structural Basis for Calmodulin as a Dynamic Calcium Sensor. *Structure* **2012**, *20*, 911–923.
- (59) Wu, G. R.; Gao, Z. Y.; Dong, A. C.; Yu, S. N. Calcium-Induced Changes in Calmodulin Structural Dynamics and Thermodynamics. *Int. J. Biol. Macromol.* **2012**, *50*, 1011–1017.
- (60) Evenas, J.; Forsen, S.; Malmendal, A.; Akke, M. Backbone Dynamics and Energetics of a Calmodulin Domain Mutant Exchanging between Closed and Open Conformations. *J. Mol. Biol.* **1999**, *289*, 603–617.
- (61) Chou, J. J.; Li, S. P.; Klee, C. B.; Bax, A. Solution Structure of Ca^{2+} -Calmodulin Reveals Flexible Hand-like Properties of Its Domains. *Nat. Struct. Biol.* **2001**, *8*, 990–997.
- (62) Masino, L.; Martin, S. R.; Bayley, P. M. Ligand Binding and Thermodynamic Stability of a Multidomain Protein, Calmodulin. *Protein Sci.* **2000**, *9*, 1519–1529.
- (63) Rabl, C. R.; Martin, S. R.; Neumann, E.; Bayley, P. M. Temperature Jump Kinetic Study of the Stability of Apo-Calmodulin. *Biophys. Chem.* **2002**, *101–102*, 553–564.
- (64) Kumar, S.; Boehm, J.; Lee, J. C. P38 MAP Kinases: Key Signalling Molecules as Therapeutic Targets for Inflammatory Diseases. *Nat. Rev. Drug Discovery* **2003**, *2*, 717–726.
- (65) Pargellis, C.; Tong, L.; Churchill, L.; Cirillo, P. F.; Gilmore, T.; Graham, A. G.; Grob, P. M.; Hickey, E. R.; Moss, N.; Pav, S.; Regan, J. Inhibition of P38 MAP Kinase by Utilizing a Novel Allosteric Binding Site. *Nat. Struct. Biol.* **2002**, *9*, 268–272.
- (66) Regan, J.; Breitfelder, S.; Cirillo, P.; Gilmore, T.; Graham, A. G.; Hickey, E.; Klaus, B.; Madwed, J.; Moriak, M.; Moss, N.; et al. Pyrazole Urea-Based Inhibitors of P38 MAP Kinase: From Lead Compound to Clinical Candidate. *J. Med. Chem.* **2002**, *45*, 2994–3008.
- (67) Huang, Y. M. M.; Chen, W.; Potter, M. J.; Chang, C. E. A. Insights from Free-Energy Calculations: Protein Conformational Equilibrium, Driving Forces, and Ligand-Binding Modes. *Biophys. J.* **2012**, *103*, 342–351.
- (68) Lovera, S.; Sutto, L.; Boubeva, R.; Scapozza, L.; Dolker, N.; Gervasio, F. L. The Different Flexibility of c-Src and c-Abl Kinases Regulates the Accessibility of a Druggable Inactive Conformation. *J. Am. Chem. Soc.* **2012**, *134*, 2496–2499.
- (69) Berteotti, A.; Cavalli, A.; Branduardi, D.; Gervasio, F. L.; Recanatini, M.; Parrinello, M. Protein Conformational Transitions: The Closure Mechanism of a Kinase Explored by Atomistic Simulations. *J. Am. Chem. Soc.* **2009**, *131*, 244–250.
- (70) Gan, W. X.; Yang, S. C.; Roux, B. Atomistic View of the Conformational Activation of Src Kinase Using the String Method with Swarms-of-Trajectories. *Biophys. J.* **2009**, *97*, L8–L10.
- (71) Filomia, F.; De Rienzo, F.; Menziani, M. C. Insights into MAPK P38 α DFG Flip Mechanism by Accelerated Molecular Dynamics. *Bioorgan. Med. Chem.* **2010**, *18*, 6805–6812.
- (72) Shan, Y. B.; Seeliger, M. A.; Eastwood, M. P.; Frank, F.; Xu, H. F.; Jensen, M. O.; Dror, R. O.; Kuriyan, J.; Shaw, D. E. A Conserved Protonation-Dependent Switch Controls Drug Binding in the Abl Kinase. *Proc. Natl. Acad. Sci. U.S.A.* **2009**, *106*, 139–144.
- (73) Kottalam, J.; Case, D. Langevin Modes of Macromolecules: Applications to Crambin and DNA Hexamers. *Biopolymers* **1990**, *29*, 1409–1421.
- (74) Hayward, J. A.; Smith, J. C. Temperature Dependence of Protein Dynamics: Computer Simulation Analysis of Neutron Scattering Properties. *Biophys. J.* **2002**, *82*, 1216–1225.
- (75) Levy, R.; Srinivasan, A.; Olson, W.; McCammon, J. Quasi-Harmonic Method for Studying very Low Frequency Modes in Proteins. *Biopolymers* **1984**, *23*, 1099–1112.
- (76) Hayward, S.; Kitao, A.; Gō, N. Harmonicity and Anharmonicity in Protein Dynamics: A Normal Mode Analysis and Principal Component Analysis. *Proteins* **1995**, *23*, 177–186.
- (77) Hayward, S.; Kitao, A.; Gō, N. Harmonic and Anharmonic Aspects in the Dynamics of BPTI: A Normal Mode Analysis and Principal Component Analysis. *Protein Sci.* **1994**, *3*, 936–943.
- (78) Hayward, S.; Go, N. Collective Variable Description of Native Protein Dynamics. *Annu. Rev. Phys. Chem.* **1995**, *46*, 223–250.
- (79) Kitao, A.; Gō, N. Conformational Dynamics of Polypeptides and Proteins in the Dihedral Angle Space and in the Cartesian Coordinate Space: Normal Mode Analysis of deca-Alanine. *J. Comput. Chem.* **1991**, *12*, 359–368.
- (80) Zheng, W. Anharmonic Normal Mode Analysis of Elastic Network Model Improves the Modeling of Atomic Fluctuations in Protein Crystal Structures. *Biophys. J.* **2010**, *98*, 3025–3034.
- (81) Vogtherr, M.; Saxena, K.; Hoelder, S.; Grimme, S.; Betz, M.; Schieborr, U.; Pescatore, B.; Robin, M.; Delarbre, L.; Langer, T.; et al. NMR Characterization of Kinase P38 Dynamics in Free and Ligand-bound Forms. *Angew. Chem., Int. Ed.* **2006**, *45*, 993–997.